Boundary Element Design Sensitivity Analysis of Symmetric Bodies

Sunil Saigal*
Carnegie Mellon University, Pittsburgh, Pennsylvania
and
R. Aithal†
Worcester Polytechnic Institute, Worcester, Massachusetts
and
Carl T. Dyka‡
General Dynamics, Groton, Connecticut

Introduction

IN obtaining solutions using numerical techniques, it is a common practice to model and analyze only a part of the actual geometry for problems having geometric and loading symmetry. This may present difficulties for an analysis using the boundary element method. First, a symmetric model usually contains a discontinuity in geometry (a corner) at the intersection of the plane of symmetry with the boundary of the object being modeled. Such discontinuities can result in inaccuracies with the boundary element method if they are not modeled correctly. Second, a symmetric axis of large length may be adjacent to a boundary of small length. This may result either in boundary elements with large dimensions existing close to those with small dimensions, or in a fine discretization of a portion of the symmetric axis lying adjacent to the boundary. Whereas the former may result in a poor conditioning of the system matrices, the latter will result in an excessive number of elements, leading to higher computer memory and storage requirements. These difficulties may be overcome in the boundary element analysis through the reflection of nodes about the axes of symmetry. This technique has been extended in this Note for the design sensitivity analysis of symmetric bodies using the boundary element method. The accuracy of results for such applications is very important for their successful use in the shape optimization process. The concept of reflection about the symmetric axes is formulated for design sensitivity analysis. This leads to a number of advantages: 1) Only that portion of the boundary which lies on one side of the symmetric plane, not including the line (surface) of symmetry, needs to be modeled, resulting in considerable savings in preprocessing efforts and time. 2) The resulting system matrices for solution are smaller in size. They require less computer memory and time, both for numerical computation of the matrix entries and for factorization of these matrices, and involve smaller round-off errors. 3) The poor conditioning of system matrices is avoided, since uneven-sized elements that may be needed when modeling the axes of symmetry, as explained earlier, are not required. Finally accurate results for sensitivities are obtained at the intersection of the symmetry planes with the boundary of the continua. Numerical results have been obtained for some examples to demonstrate the accuracy and efficiency obtained using the symmetry plane reflection property.

Received Jan. 13, 1989; revision received May 10, 1989.

*Assistant Professor, Mechanical Engineering Department, Associate Member AIAA.

†Graduate Research Assistant, Mechanical Engineering Department.

‡Engineering Specialist, Electric Boat Division.

Theoretical Development

The boundary element equations, based on Somigliana's identity, can be expressed as[1]

$$[H]\{U\} = [G]\{T\} + \{f\} \tag{1}$$

$$[H] = \sum_{k=1}^{N} \int_{-1}^{+1} [t^*][h]J\,\mathrm{d}\xi, \qquad [G] = \sum_{k=1}^{N} \int_{-1}^{+1} [u^*][h]J\,\mathrm{d}\xi$$

The implicit differentiation of Eq. (1) with respect to the design variable X_L leads to the boundary element design sensitivity analysis equations as[2]

$$[H]\{U\}_{,L} = [G]_{,L}\{T\} + [G]\{T\}_{,L} - [H]_{,L}\{U\} + \{f\}_{,L} \tag{2}$$

where $\{U\}$ and $\{T\}$ are the vectors of displacements and tractions, respectively; $[H]$ and $[G]$ are the boundary element system matrices; $[h]$ is a matrix containing the interpolation functions; J is the Jacobian; $\{f\}$ is the vector accounting for body forces[3]; $(\,)_{,L}$ denotes differentiation of $(\,)$ with respect to X_L; N is the number of boundary elements; and the supescript * denotes the fundamental solutions.

Consider the symmetric structure shown in Fig. 1a. The lk entries of $[H]$ and $[G]$ for the load point at i and the field point at Q are written as

$$H_{lk}^{iQ} = \int_{\xi=-1}^{+1} t_{lk}^{*}[r^{iQ}(\xi)]h_Q(\xi)J(\xi)\,\mathrm{d}\xi \tag{3}$$

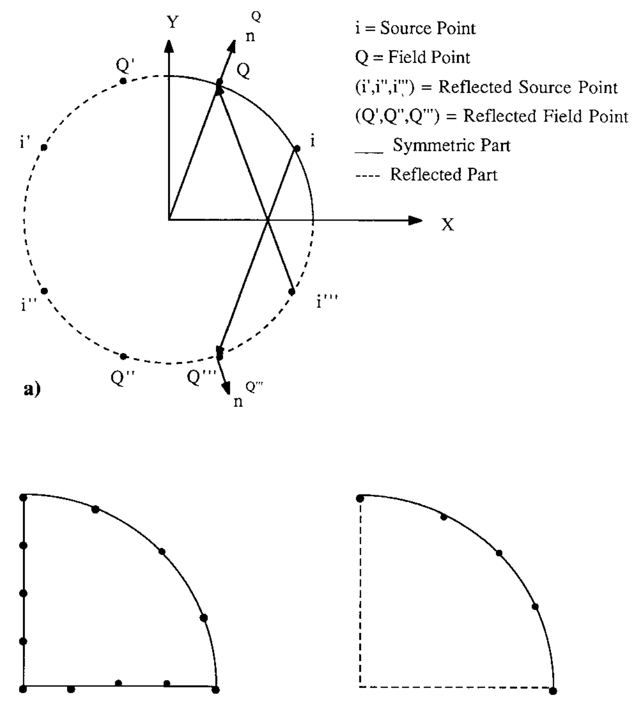

Fig. 1 a) Two-dimensional elasticity double symmetry about $x=0$ and $y=0$; b) mesh for the case without reflection; c) mesh for the case with reflection.

$$G_{lk}^{iQ} = \int_{\xi=-1}^{+1} u_{lk}^{*} [r^{iQ}(\xi)] h_Q(\xi) J(\xi) \, d\xi \tag{4}$$

where $r^{iQ}(\xi)$ is the distance from the source point i to the integration point ξ within the element being integrated. Similar entries for the sensitivity matrices $[H]_{,L}$ and $[G]_{,L}$ are given as

$$H_{lk,L}^{iQ} = \int_{\xi=-1}^{+1} \Big[t_{lk,L}^{*} [r^{iQ}(\xi)] h_Q(\xi) J(\xi) + t_{lk}^{*}[r^{iQ}(\xi)] h_Q(\xi) J_L(\xi) \Big] d\xi \tag{5}$$

$$G_{lk,L}^{iQ} = \int_{\xi=-1}^{+1} \Big[u_{lk,L}^{*} [r^{iQ}(\xi)] h_Q(\xi) J(\xi) + u_{lk}^{*}[r^{iQ}(\xi)] h_Q(\xi) J_L(\xi) \Big] d\xi \tag{6}$$

In the boundary element procedure, the contributions $(\ )_{lk}^{iQ}$ are computed for i located successively at all of the boundary element nodal points and for Q also successively located at all of the boundary element nodal points. If the symmetric part of the structure is considered, one approach is to model the axes of symmetry, as shown in Fig. 1b. Instead, however, for boundary elements it is sufficient to model only the symmetric part of the structure indicated in Fig. 1c by the solid line. The axes of symmetry ($x=0$ and $y=0$ in this case) need not be discretized.[4]

In Eq. (1) the expanded form of the row corresponding to the source point i is of the form

$$\begin{aligned}
&(H^{i1}\underline{u}^1 + H^{i2}\underline{u}^2 + - - - + H^{im}\underline{u}^m) \\
&+ (H^{i1'}\underline{u}^{1'} + H^{i2'}\underline{u}^{2'} + - - - + H^{im'}\underline{u}^{m'}) \\
&+ (H^{i1''}\underline{u}^{1''} + H^{i2''}\underline{u}^{2''} + - - - + H^{im''}\underline{u}^{m''}) \\
&+ (H^{i1'''}\underline{u}^{1'''} + H^{i2'''}\underline{u}^{2'''} + - - - + H^{im'''}\underline{u}^{m'}) \\
&= (G^{i1}\underline{t}^1 + G^{i2}\underline{t}^2 + - - - + G^{im}\underline{t}^m) \\
&+ G^{i1'}\underline{t}^{1'} + G^{i2'}\underline{t}^{2'} + - - - + G^{im'}\underline{t}^{m'}) \\
&+ (G^{i1''}\underline{t}^{1''} + G^{i2''}\underline{t}^{2''} + - - - + G^{im''}\underline{t}^{m''}) \\
&+ (G^{i1'''}\underline{t}^{1'''} + G^{i2'''}\underline{t}^{2'''} + - - - + G^{im'''}\underline{t}^{m'''})
\end{aligned} \tag{7}$$

where i', i'', and i''' are the reflected source points; Q', Q'', and Q''' are the reflected field points as in Fig. 1a; the underbar (_) denotes matrices; the superscript pair ij refers to the source point i/field point j pair; and $\underline{u} = \lfloor u_x u_y \rfloor$. Because of double symmetry, we have

$$u_x^{i'} = -u_x^i, \qquad u_y^{i'} = u_y; \qquad u_x^{i''} = -u_x^i,$$

and

$$u_y^{i''} = -u_y^i \qquad u_x^{i'''} = u_x^i, \qquad u_y^{i'''} = -u_y^i \tag{8}$$

Combining Eqs. (7) and (8), we get

$$\begin{aligned}
&(H^{i1} \pm H^{i1'} \pm H^{i1''} \pm H^{i1'''})\underline{u}^1 + - - \\
&+ (H^{im} \pm H^{im'} \pm H^{im''} \pm H^{im'''})\underline{u}^m \\
&= (G^{i1} \pm G^{i1'} \pm G^{i1''} \pm G^{i1'''})\underline{t}^1 + - - \\
&+ (G^{im} \pm G^{im'} \pm G^{im''} \pm G^{im'''})\underline{t}^m
\end{aligned} \tag{9}$$

in which the + or − indicates sign changes in some of the components of the matrices. From Eq. (9), it is seen that the evaluation of the various H and G terms still requires the reflected geometry denoted by primes. It can be rewritten so that only the symmetric part of the geometry is involved.

In Eqs. (3) and (4), the fundamental solutions denoted by *are given, for example, for the two-dimensional displacement case as

$$u_{lk}^{*}(r^{iQ'}) = \frac{1}{8\pi G(1-\nu)} \left[(3-4\nu) \ \ell n\left(\frac{1}{r^{iQ'}}\right) \delta_{lk} + \frac{\partial r^{iQ'}}{\partial x_l} \frac{\partial r^{iQ'}}{\partial x_k} \right) \tag{10a}$$

where

$$\frac{\partial r^{iQ'}}{\partial x_l} = \frac{1}{r^{iQ'}} (r_{x_l}^{iQ'}) \tag{10b}$$

Because of symmetry, $r^{iQ'} = r^{i'Q}$, $r_x^{iQ'} = -r_x^{i'Q}$, and $r_y^{iQ'} = r_y^{i'Q}$. Substituting these relations in Eq. (10), we see that

$$u_{11}^{*}(r^{iQ'}) = u_{11}^{*}(r^{i'Q}) \tag{11a}$$

$$u_{12}^{*}(r^{iQ'}) = u_{21}^{*}(r^{iQ'}) = -u_{12}^{*}(r^{i'Q}) \tag{11b}$$

$$u_{22}^{*}(r^{iQ'}) = u_{22}^{*}(r^{i'Q}) \tag{11c}$$

Then from Eqs. (3) and (11) it can be seen that

$$H^{iQ'} = \pm H^{i'Q} \tag{12}$$

and, similarly, it can be shown that

$$G^{iQ'} = \pm G^{i'Q} \tag{13}$$

Extending the same technique for the reflected portions ($''$), ($'''$), Eq. (9) can now be written in terms of only the symmetric geometry as

$$\begin{aligned}
&(H^{i1} \pm H^{i'1} \pm H^{i''1} \pm H^{i'''1})\underline{u}^1 + - \\
&+ (H^{im} \pm H^{i'm} \pm H^{i''m} \pm H^{i'''m})\underline{u}^m \\
&= (G^{i1} \pm G^{i'1} \pm G^{i''1} \pm G^{i'''1})\underline{t}^1 + - - \\
&+ G^{im} \pm G^{i'm} \pm G^{i''m} \pm G^{i'''m})\underline{t}^m
\end{aligned} \tag{14}$$

where proper care must be taken in prescribing the signs + and −. Consider now a term within a parenthesis in Eq. (14), say, $(G^{im} \pm G^{i'm} \pm G^{i''m} \pm G^{i'''m})$. Each of the constituting terms G^{im}, $G^{i'm}$, $G^{i''m}$, and $G^{i'''m}$ requires the computation of an integration as given in Eq.(4). However, since these terms involve the same field point at m, they can be computed together in one integration using relations of the type shown in Eq. (11) as

$$(G_{lk}^{im} \pm G_{lk}^{i'm} \pm G_{lk}^{i''m} \pm G_{lk}^{i'''m}) = \int_{-1}^{+1} \Big[\Big\{ u_{lk}^{*}(r^{im}) \pm u_{lk}^{*}(r^{i'm}) \pm u_{lk}^{*}(r^{i''m}) \pm u_{lk}^{*}(r^{i'''m}) \Big\} h_m(\xi) J(\xi) \Big] d\xi \tag{15}$$

The original source point i is always closer to the element being integrated than any of the reflected nodes i', i'', or i'''. Thus, the same integration rule can be used for the reflected nodes as required by the original node. We note that, when the i is within the element being integrated, special integration procedures must be employed. Thus, evaluation of the G_{lk}^{im} and H_{lk}^{im} terms must be done separately. However, since the reflected source points are all still outside the element for double symmetry, they can all be grouped together, as indicated in Eq. (15). By performing the differentiation of the expressions of the type shown in Eq. (11) with respect to the X_L, expressions corresponding to Eq. (15) for design sensitivity analysis can also be developed. The preceding developments can be extended for three-dimensional analyses using similar arguments.

Numerical Results

The improvement in accuracy and the savings in computer time and memory obtained for symmetric bodies for design sensitivity analysis results using the formulations described in the preceding section are demonstrated through numerical examples. The examples studied are 1) an infinite plate with an elliptic hole subjected to an axial tension of 100 psi, 2) a circular plate with a circular hole under external pressure of 100 psi, and 3) a circular rod under self-weight. The geometric dimensions and material properties for these examples are shown in Fig. 2. The first two examples were solved using two-dimensional continuous quadratic boundary elements, and the third example was solved using three-dimensional continuous triangular elements with eight nodes. Each example was solved by modeling only the symmetric part of the structure. In each of the examples, the results were obtained for two cases: 1) for QS the lines of symmetry were modeled and the reflection of the source point was not considered, and 2) for QSR the lines

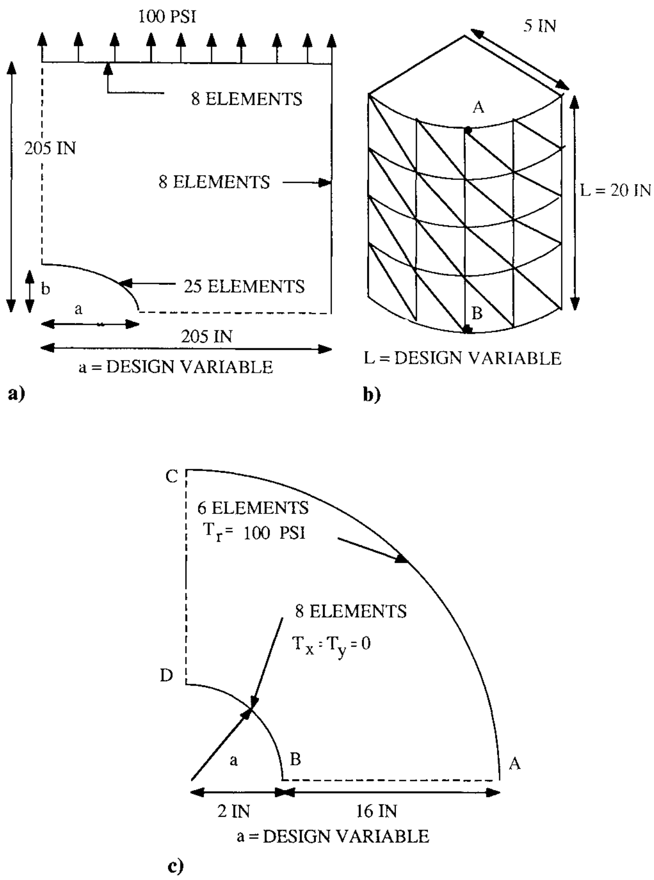

Fig. 2 a) Elliptic hole in an infinite plate; b) circular rod in quarter symmetry; c) circular hole in a circular plate under external pressure.

Table 1 Case studies for comparison of accuracy of sensitivities using symmetry with and without using reflection property

Elliptical hole in an infinite plate

	Location A		Location B	
	du_y/db, 10^{-6}	$d\sigma_{11}/db$	du_y/db, 10^{-6}	$d\sigma_{11}/db$
$a/b = 8.0$				
Analytical	6.0000	0.000	3.0000	200.00
QSR[a]	6.1099	−0.079	3.0629	199.68
QS[b]	6.1503	−0.012	3.0684	209.93
$a/b = 4.0$				
Analytical	6.0000	0.000	3.0000	200.00
QSR	6.0786	0.043	3.0416	200.13
QS	6.0773	−0.135	3.0274	198.48

Circular plate under external pressure

	Location A		Location B	
Analysis type	du_x/db, 10^{5}	$d\sigma_{yy}/db$	du_x/db, 10^{-5}	$d\sigma_{yy}/db$
Analytical	1.3604	2.041	6.8701	2.041
QSR	1.3585	2.037	6.8626	3.294
QS	1.3598	2.041	6.8690	3.294

Circular rod under self-weight

	Location A		Location B	
Analysis type	du_z/db, 10^{-2}	$d\sigma_{zz}/db$	du_z/db, 10^{-2}	$d\sigma_{zz}/db$
Analytical	0.0	2318.4	0.1546	0.0
QSR	0.0	2319.2	0.1545	0.0
QS	0.0	2317.8	0.1545	0.0

[a]Quarter symmetry with reflection. [b]Quarter symmetry.

Table 2 Case studies for comparison of model size, storage, and CPU timing using symmetry with and without using reflection property

	QS	QSR
Elliptic hole in an infinite plate		
Number of elements	124	41
Number of nodes	248	84
CPU time for sensitivity analysis, s	496.62	154.4
Design variable, s	884.88	252.6
Circular plate under external pressure		
Number of elements	32	14
Number of nodes	64	30
CPU time for sensitivity analysis, s	60.18	48.66
Total time of analysis for one design variable, s	102.5	76.60
Circular rod under self-weight		
Number of elements	248	120
Number of nodes	498	273
Core memory required[a]	3.328	1.0

[a]Expressed as a ratio of memory used for QSR analysis.

of symmetry were not modeled and the reflection of the source point was considered. The results for the design sensitivity analysis for these examples are given in Table 1 for both QS and QSR analyses. The exact values of sensitivities obtained through the differentiation of the elasticity response expressions were also given in this table for comparison of accuracies. A significant improvement in accuracy was seen at the junction of the boundary of the solid with the line of symmetry. For example, for the infinite plate with an elliptic hole, the QS analysis gives a sensitivity $d\sigma_{11}/db$ of 209.93, and the QSR gives a value of 199.68 compared to the exact value of 200. Similar improvements in the other results were also seen. The savings in computations obtained by the use of the QSR analysis are shown in Table 2 for the three examples studied. The computing timings shown were obtained for the RIDGE 3200 computer system at Worcester Polytechnic Institute. It was observed that substantial economy can be obtained even for the case of one design variable. For real problems involving multiple design variables, the present approach is very promising for efficient and accurate design sensitivity analysis of structures exhibiting symmetry.

References

[1]Banerjee, P. K. and Butterfield, R., *Boundary Element Methods in Engineering Science,* McGraw-Hill, London, 1981.

[2]Saigal, S., Aithal, R., and Kane, J. H., "Conforming Boundary Elements in Plane Elasticity for Shape Design Sensitivity," *International Journal for Numerical Methods in Engineering* (to be published).

[3]Pape, D. A. and Banerjee, P. K., "Treatment of Body Forces in 2D Elastostatic BEM Using Particular Integrals," *Journal of Applied Mechanics,* Vol. 54, Dec. 1987, pp. 866–871.

[4]Banerjee, P. K., Ahmad, S., and Chen, K., "Advanced Application of BEM to Wave Barriers in Multi-Layered Three-Dimensional Soil Media," *Earthquake Engineering and Structural Dynamics*, Vol. 16, Oct. 1988, pp. 1041–1060.